Chem. Res. Chinese Universities, 2019, 35(1), 133—138 doi: 10.1007/s40242-019-8097-5

Effects of Cerium Oxides on the Catalytic Performance of Pd/CNT for Methanol Oxidation

CHEN Weimin[1*], ZHANG Yu[1] and ZHU Zhenyu[1,2]

1. School of Environmental and Chemical Engineering, Shenyang Ligong University, Shenyang 110159, P. R. China;

2. R & D Center of Shandong Shinlong Group, Shouguang 262709, P. R. China

Abstract The carbon nanotubes supported palladium(Pd/CNT) nanocatalysts were modified by cerium oxides/hydroxides and their catalytic performances for methanol oxidation were evaluated. Electrochemical measurements indicate that the introduction of cerium remarkably improves the catalytic activity of Pd/CNT catalysts towards methanol oxidation. X-Ray photoelectron spectra results reveal an interaction between palladium and cerium oxides. It is also observed that cerium-modified catalysts have excellent poison resistances, which is attributed to the poison-removal ability of cerium oxides/hydroxides. The highly oxidized cerium oxides/hydroxides have a strong ability to inhibit the accumulation of carbonaceous intermediates on the active sites of Pd catalysts.

Keywords Electrocatalyst; Methanol oxidation; Palladium; Cerium; Modification

1 Introduction

The alkaline direct alcohol fuel cells(ADAFCs) attract much attention recently[1—4]. In alkaline media, the main electrocatalysts for alcohol oxidation are Pd-based catalysts. Because ADAFCs operate at relatively low temperatures, the overpotentials of alcohol oxidation are often high in both anode and cathode. In addition, the carbonaceous intermediates tend to accumulate at active sites of catalysts, resulting in catalyst poisonings. In order to overcome those problems, enormous efforts have been devoted. For instance, transition metals and metal oxides, such as Ni[5,6], Au[7,8], Co[9,10], Mo[11,12], Ru[13,14], Ir[15], Cu[16], Rh[17], Ag[18], V[19] and Mn[20] have been employed to modify Pd-based nanocatalysts.

Cerium is outstanding in promoting the performances of noble metal catalysts due to its variable oxidation states. Ou and co-workers[21] observed a strong Pt-ceria interaction related to the redox reaction between Pt and CeO_2, which contributed to the improved catalytic performances. On the other hand, the effects of cerium oxides/hydroxides can also be explained by a bifunctional mechanism[22,23]. The OH_{ad} species on the surface of cerium oxide transform CO-like poisoning species(CO_{ad}) to CO_2, releasing the active sites on Pt surface for further electrochemical reaction. The influences of cerium on PtRu catalysts[24] and Pd catalysts[25,26] were also reported. Sun and co-workers[27] observed that cerium can switch between Ce(IV) and Ce(III) in cerium oxide, and this process can be accelerated by noble metals, such as platinum, resulting in more oxygen vacancies on the surface. In this study, cerium oxides/hydroxides were treated at different temperatures, and the catalytic performances of the prepared PdCe catalysts were evaluated. The results indicate that the addition of cerium remarkably increases the catalytic activities of Pd catalysts for methanol oxidation. In addition, the poison resistances of Pd catalysts are improved due to the poison-removal ability of cerium oxides/hydroxides.

2 Experimental

2.1 Preparation of Ce/CNT

Treated multiwalled carbon nanotubes(160 mg, purchased from Chengdu Organic Chemicals Co., Ltd., and treated with 6 mol/L H_2SO_4-HNO_3 solution at 110 °C for 3 h) were suspended in 80 mL of deionized water, then 4.4 mL of cerium nitrate solution(1.07 mg Ce/mL) was added to the suspension. An appropriate amount of sodium borohydride solution was added to the suspension dropwise under vigorous agitation. The pH value of the suspension was adjusted to 9—10 by adding 1 mol/L sodium hydroxide solution. The suspension was agitated at 25 °C for 4 h. The mixture was filtered and washed with deionized water, and then heated in a tube furnace at 200 or 350 °C for 3 h. The obtained carbon nanotubes supported cerium oxides/hydroxides were designated as Ce/CNT200 and Ce/CNT350, respectively.

2.2 Preparation of PdCe/CNT

The 20%(mass fraction) PdCe/CNT catalysts were synthesized using an ethylene glycol(EG) reduction method[28]. The molar ratio of Pd:Ce was 10:1. The prepared Ce/CNT200 or Ce/CNT350 was suspended in 60 mL of EG solution ultrasonically for 30 min, then 14.8 mL of the palladium chloride

*Corresponding author. Email: cwmchem@163.com

Received March 26, 2018; accepted September 14, 2018.

Supported by the National Natural Science Foundation of China(No.21273152).

(Sinopharm Chemical Reagent Co., Ltd., China) EG solution (2.38 mg Pd/mL) was added to the suspension dropwise. The pH value of the suspension was adjusted to 10 by adding 1 mol/L sodium hydroxide solution. The mixture was refluxed in an oil bath at 130 °C for 3 h. Afterward, the mixture was filtered and washed with deionized water, then dried at 70 °C in a vacuum oven for 24 h. The obtained catalysts were designated as PdCe/CNT200 and PdCe/CNT350, respectively. For comparison, Pd/CNT was synthesized in the same way.

2.3 Characterization

Transmission electron microscopy(TEM) investigations were carried out using a JEOL JEM-2000EX microscope operating at 120 kV. X-Ray diffraction(XRD) measurements were performed on an X'Pert PRO X-ray diffractometer using Cu $K\alpha$ radiation with a Ni filter. The tube voltage was maintained at 40 kV, and the tube current was at 40 mA. The 2θ angular region between 20° and 85° was explored at a scan rate of 5°/min, with the resolution of 0.02°. The differential thermal analysis(DTA) was conducted using a DTA-100 differential thermal analyzer (Beijing Henven Scientific Instrument, China). X-Ray photoelectron spectra(XPS) were collected on a Thermo VG ESCALAB250 multifunction surface analysis system with a monochromatic aluminum $K\alpha$(1486.6 eV) X-ray source operating at 150 W.

Electrochemical measurements were conducted at 25 °C, using a three-electrode system. The working electrode was a glassy carbon electrode with a diameter of 4 mm. A Pt foil and a saturated calomel electrode(SCE) served as the counter electrode and the reference electrode, respectively. Catalyst inks were made by mixing 5 mg of the catalyst with 50 μL of 5%(mass fraction) Nafion® ionomer solution(DuPont Corp.) and 1 mL of ethanol ultrasonically for 30 min. In electrode preparation, 25 μL of the prepared catalyst slurry was pipetted onto the glassy carbon electrode, and the solvent was evaporated. Electrochemical measurements were conducted using a Gamry Reference 3000 potentiostat/galvanostat. For electrochemical impedance spectroscopy(EIS) measurements, impedance spectra were recorded at five points per decade by superimposing a 5 mV alternating current signal on the cell under potentiostatic mode over the frequency range from 100 kHz to 0.1 Hz. The applied potential was –0.25 V *vs.* SCE.

3 Results and Discussion

TEM images of electrocatalysts are shown in Fig.1. It can be seen that cerium-modified catalysts, *i.e.*, PdCe/CNT200 and PdCe/CNT350, exhibit more uniform distributions of metal particles over the surfaces of CNTs, as compared to Pd/CNT.

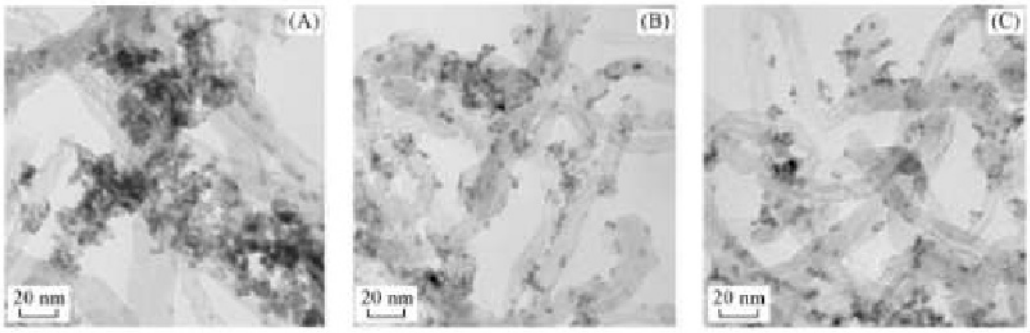

Fig.1 TEM images of catalysts Pd/CNT(A), PdCe/CNT200(B) and PdCe/CNT350(C)

XRD patterns of catalyst samples are shown in Fig.2. The diffraction peak at 2θ=26.0° can be attributed to the hexagonal graphite structure's (002) crystal plane in carbon nanotubes. Supported Pd forms a face-centered cubic(fcc) structure and has major peaks at around 40.0°(111), 46.5°(200), 68.1°(220), and 81.9°(311). No other diffraction peaks are observed from the XRD patterns. This result implies that the cerium oxides/hydroxides exist mainly in amorphous forms. The Pd(220) peak was selected to calculate the mean crystallite sizes of catalyst particles because it is isolated from the diffraction peaks of the carbon support. The crystallite sizes of catalysts were determined according to Scherrer's formula[29]. The calculated mean crystallite sizes of Pd/CNT, PdCe/CNT200 and PdCe/CNT350 are 2.9, 3.0 and 3.2 nm, respectively. This result is in good agreement with the TEM result. It is inferred that cerium oxides/hydroxides in PdCe/CNT200 and PdCe/CNT350 hinder the agglomeration of Pd nanoparticles to some extent during the preparation.

It is noteworthy that the diffraction peaks of PdCe/CNT200 and PdCe/CNT350 appear at slightly lower 2θ angles as compared to that of Pd/CNT. For instance, the Pd(220) peaks of PdCe/CNT200 and PdCe/CNT350 appear at 67.5° and 67.6°, respectively, while the Pd(220) peak of Pd/CNT appears at 68.1°. This could be ascribed to the existence of cerium species in cerium-modified Pd catalysts.

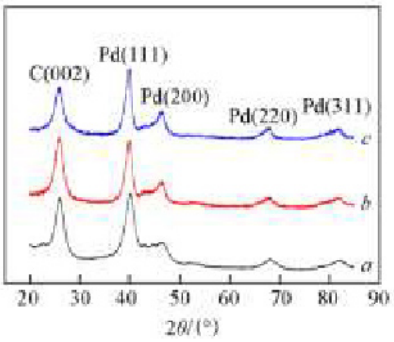

Fig.2 XRD patterns of catalysts Pd/CNT(*a*), PdCe/CNT200(*b*) and PdCe/CNT350(*c*)

Fig.3(A) shows the cyclic voltammetry(CV) curves of catalysts recorded in 1.0 mol/L KOH solution. The peaks within the potential region of –1.00—–0.65 V are assigned to the hydrogen adsorption/desorption. It is seen that the hydrogen

adsorption/desorption peaks of PdCe/CNT200 and PdCe/CNT350 are larger than that of Pd/MWCNT. This could be explained by the promoting effect of cerium oxide on the hydrogen spillover on the catalyst surface, as revealed by Zhou and co-workers[30]. The potential region within –0.65—–0.45 V is assigned to the double electric layer region. It can be seen that PdCe/CNT200 and PdCe/CNT350 have remarkably larger double layer capacitances than Pd/CNT. This could be explained by the rough cerium oxides/hydroxides surfaces of PdCe/CNT200 and PdCe/CNT350.

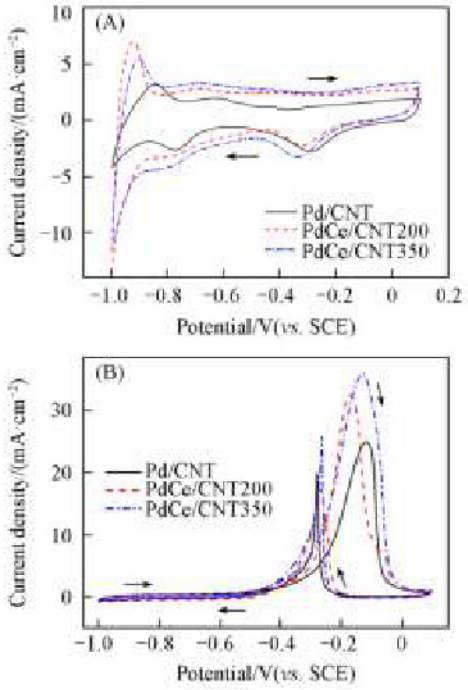

Fig.3 CV curves of catalysts recorded in 1.0 mol/L KOH solution(A) and 1.0 mol/L CH_3OH-1.0 mol/L KOH solution(B) at a scan rate of 20 mV/s

Fig.3(B) shows the cyclic voltammetry(CV) curves of catalysts recorded in 1.0 mol/L CH_3OH-1.0 mol/L KOH solution. The forward anodic peak is assigned to the oxidation of methanol and the backward oxidation peak is assigned to the oxidation of carbonaceous species formed during the forward oxidation scan. The peak current densities of PdCe/CNT200 and PdCe/CNT350 in the forward scan are measured to be 32.5 and 35.9 mA/cm^2, respectively, significantly higher than that of Pd/CNT(24.9 mA/cm^2). This result indicates that the introduction of cerium improved the catalytic activity of Pd catalysts.

Fig.4 shows the linear sweep voltammetry(LSV) curves of catalysts recorded in 1.0 mol/L CH_3OH-1.0 mol/L KOH solution. It is seen that the onset potentials for methanol oxidation(defined as the potential values corresponding to the current density of 2.50 mA/cm^2) of PdCe/CNT200 and PdCe/CNT350 are –0.340 and –0.348 V, respectively, remarkably lower than that of Pd/CNT(–0.322 V). This result implies that PdCe/CNT200 and PdCe/CNT350 have lower overpotentials than Pd/CNT, which could be explained by the interaction between palladium and cerium oxides/hydroxides, as reported by Tauster and co-workers[31,32].

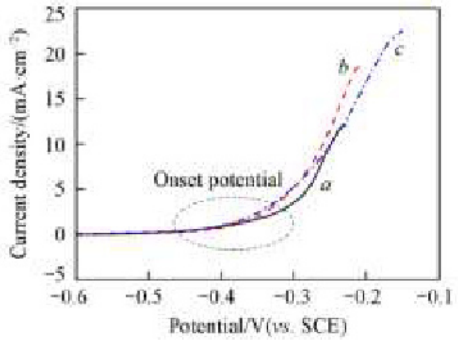

Fig.4 LSV curves of catalysts recorded in 1.0 mol/L CH_3OH-1.0 mol/L KOH solution at a scan rate of 1 mV/s

a. Pd/CNT; *b*. PdCe/CNT200; *c*. PdCe/CNT350.

The EIS of catalysts recorded in 1.0 mol/L CH_3OH-1.0 mol/L KOH solution are shown in Fig.5(A). The Nyquist diagram consists of two arcs. The small arc that appears in the high frequency range relates to electrical conduction *via* the electrical double layer or geometric boundaries[33,34]. The arc that appears in the low frequency range relates to the electro-oxidation of methanol, and at the low frequency end, this arc extends into the fourth quadrant and forms an induction loop that represents the electro-oxidation of CO_{ad}[35,36].

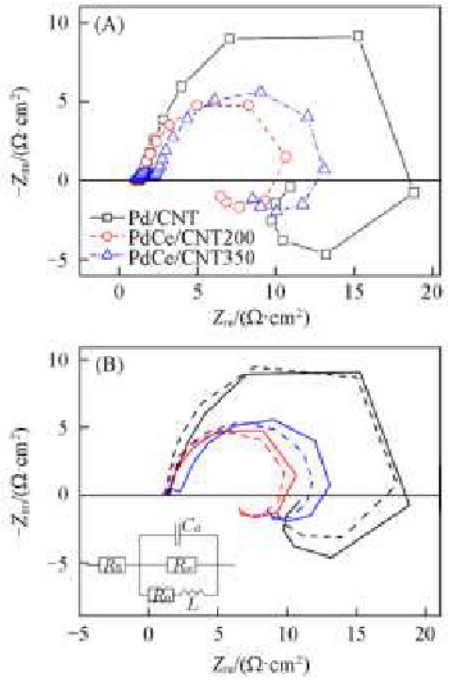

Fig.5 EIS spectra of catalysts in 1.0 mol/L CH_3OH-1.0 mol/L KOH solution(A) and the fitting results of the EIS spectra(B)

(B) The solid lines: the EIS curves; the dash lines: the fitting curves. Inset: the equivalent circuit.

The curve-fitting results of the EIS spectra are shown in Fig.5(B). The inset of Fig.5(B) is the equivalent circuit. R_s represents the solution resistance; R_∞ is the charge transfer resistance; R_0 serves to modify the phase-delay due to the oxidation of CO_{ad}. The capacitor C_d is believed to be associated with the redistribution of charge at the anode. The inductance L can be rationalized by the relaxation of CO_{ad} coverage from the active sites. Table 1 shows the fitting results of the EIS spectra.

It is seen that the charge transfer resistances R_∞ in PdCe/CNT200 and PdCe/CNT350 are 9.7 and 10.8 $\Omega\cdot cm^2$, respectively, considerably smaller than that of Pd/CNT(21.9 $\Omega\cdot cm^2$), indicating that cerium-modified Pd catalysts have higher catalytic activity for methanol oxidation than the unmodified one. This result is consistent with the CV curves.

Table 1 Fitting results of the EIS spectra

Catalyst	R_s/Ω	10^6C_d/F	R_0/Ω	L/H	R_∞/Ω
Pd/CNT	1.39	89	11.5	4.1	21.9
PdCe/CNT200	1.21	207	8.7	7.7	9.7
PdCe/CNT350	1.58	106	13.7	14.4	10.8

Fig.6 shows chronoamperometry(CA) curves of catalysts recorded in 1.0 mol/L CH_3OH-1.0 mol/L KOH solution. During the test, the performance loss ratios of Pd/CNT, PdCe/CNT200 and PdCe/CNT350 are 77.3%, 59.6% and 41.8%, respectively. This result indicates that PdCe/CNT200 and PdCe/CNT350 have higher electrochemical stabilities than Pd/CNT, which could be attributed to the existence of cerium oxides/hydroxides in them. In other words, the addition of cerium oxides/hydroxides improves the poison resistance of Pd catalysts. The fact that PdCe/CNT350 has a higher electrochemical stability than PdCe/CNT200 likely suggests that the cerium oxides/hydroxides in PdCe/CNT350 are different from that in PdCe/CNT200.

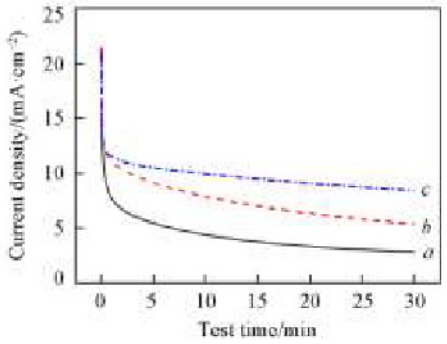

Fig.6 CA curves of catalysts recorded in 1.0 mol/L CH_3OH-1.0 mol/L KOH solution

a. Pd/CNT; *b*. PdCe/CNT200; *c*. PdCe/CNT350.

The DTA curve of the as-synthesized cerium hydroxide by the hydrolysis of cerium nitrate is shown in Fig.7. The broad peak appearing within the temperature range of 30—120 °C is attributed to the removal of the hygroscopic water. The peak appearing at 146 °C is assigned to the removal of some crystal water. The broad peak centered at approximately 299 °C could be identified as the removal of the structural hydroxyls and the

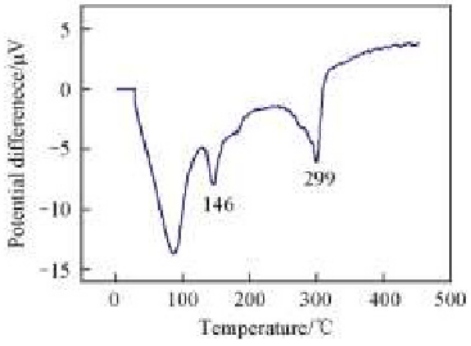

Fig.7 DTA curve of the as-prepared cerium hydroxide

deep oxidation of the cerium hydroxide[37,38] as shown in [Eq.(1)]:

$$4Ce(OH)_3+O_2\longrightarrow 4CeO_2+6H_2O \quad (1)$$

So it is inferred that after heat treatment at 200 °C, cerium exists mainly in the forms of oxides/hydroxides in relatively low oxidation states, such as $Ce(OH)_3$ or CeO(OH). In contrast, after heat treatment at 350 °C, cerium exists mainly in the forms of oxides/hydroxides in high oxidation states, such as CeO_2. Thus, the good poison resistance of PdCe/CNT350 can be attributed to the high-valence cerium oxides/hydroxides in PdCe/CNT350 as shown in Eq.(2), which accelerate the removal of CO-like carbonaceous intermediates from the active sites.

$$Pd—CO_{ad}+2CeO_2\longrightarrow Ce_2O_3+Pd+CO_2 \quad (2)$$

Fig.8(A) shows the wide survey XPS spectra of electrocatalysts. XPS peaks corresponding to C_{1s}, O_{1s}, Pd_{3d}, Pd_{3p} and Ce_{3d} spectra are observed. Fig.8(B) shows the Pd_{3d} region XPS spectra. It is seen that the Pd_{3d} peaks of PdCe/CNT200 and PdCe/CNT350 appear at higher binding energies as compared to that of Pd/CNT. It has been reported that in cerium- modified Pt catalysts, the interaction between platinum and cerium oxide led to an electron transfer from Pt to CeO_2[27,39]. Similarly, it is inferred that in cerium-modified Pd catalysts, the oxidation states of palladium are also increased *via* the synergistic effect.

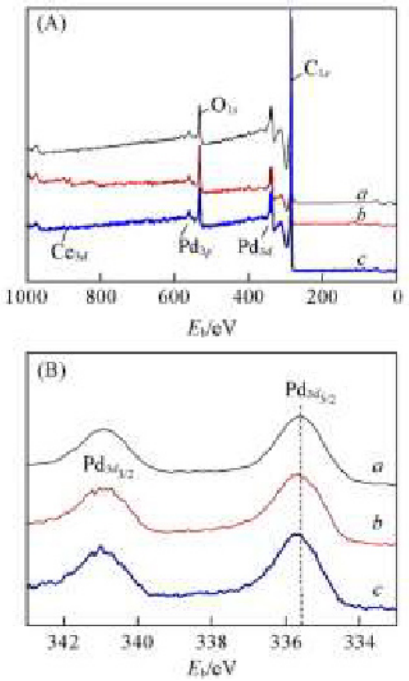

Fig.8 Wide survey(A) and Pd_{3d} region XPS spectra(B) of catalysts Pd/CNT(*a*), PdCe/ CNT200(*b*) and PdCe/CNT350(*c*)

The Pd_{3d} regions of the XPS spectra are deconvoluted, as shown in Fig.9. It indicates that Pd exists in different chemical states in the catalysts. The doublet appearing at the binding energies of 335.4 and 340.7 eV is attributed to metallic palladium Pd(0). The doublet appearing at the binding energies of 336.1 and 341.4 eV is assigned to PdO_{ad} species. The doublet appearing at the binding energies of 337.5 and 342.8 eV can be assigned to PdO species. The curve-fitting results of the $Pd_{3d_{5/2}}$ XPS spectra are shown in Table 2. The contents of Pd(0) in

PdCe/CNT200 and PdCe/CNT350 are 56.0% and 51.0%, respectively, remarkably lower than that in Pd/CNT(66.2%). This result reveals a partial electron transfer from palladium to cerium. The synergistic interaction between palladium and cerium is thought to contribute to the improved catalytic activities and poison resistances of cerium-modified Pd catalysts.

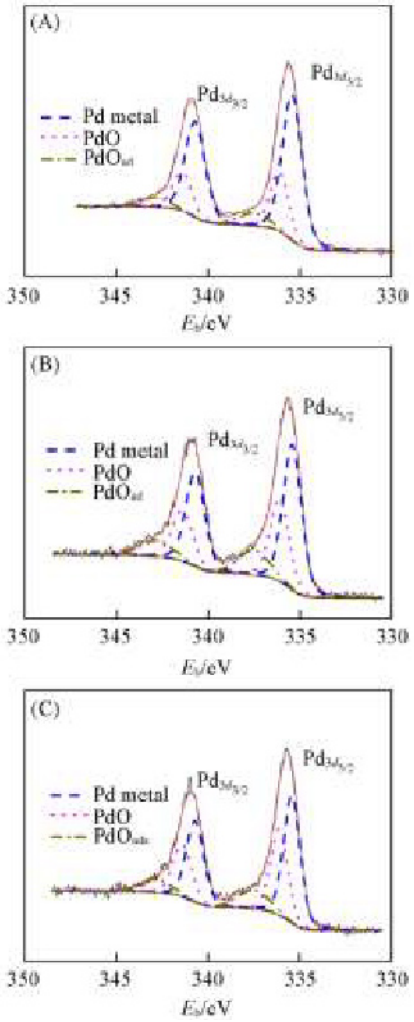

Fig.9 Deconveluted Pd_{3d} XPS spectra of catalyst samples

(A) Pd/CNT; (B) PdCe/CNT200; (C) PdCe/CNT350.

Table 2 Curve-fitting results of the $Pd_{3d_{5/2}}$ XPS spectra

Catalyst	Pd	E_b/eV	Relative ratio(%)
Pd/CNT	Pd metal	335.4	66.2
	PdO_{ad}	336.1	24.7
	PdO	337.5	9.1
PdCe/CNT200	Pd metal	335.4	56.0
	PdO_{ad}	336.1	29.6
	PdO	337.5	14.4
PdCe/CNT350	Pd metal	335.4	51.0
	PdO_{ad}	336.1	34.9
	PdO	337.5	14.1

Fig.10 shows the Ce_{3d} region of XPS spectra of electrocatalysts, which consists of two series of peaks. The peaks at 883.0, 886.2 and 898.8 eV are assigned to $Ce_{3d_{5/2}}$, while those at 901.3, 904.5 and 917.3 eV are assigned to $Ce_{3d_{3/2}}$. The ill-defined valley between 883.0 and 886.2 eV is assigned to $3d^9 4f^1(O_{2p}{}^6)$ Ce(III) state[27]. The peaks at 886.2 and 904.5 eV are typical of Ce(III)[22], which are observed to be considerably weaker in PdCe/CNT350 than in PdCe/CNT200. This result indicates that the Ce(III) content in PdCe/CNT350 is lower than that in PdCe/CNT200. Therefore, it is suggested that in PdCe/CNT350, cerium exists mainly in the forms of high-valence oxides/hydroxides such as CeO_2 or $CeO(OH)_2$, which contribute to the good poison resistance of PdCe/CNT350. The high-valence cerium oxides/hydroxides accelerate the removal of carbonaceous intermediates from the active sites so as to improve the poison resistance of Pd catalysts.

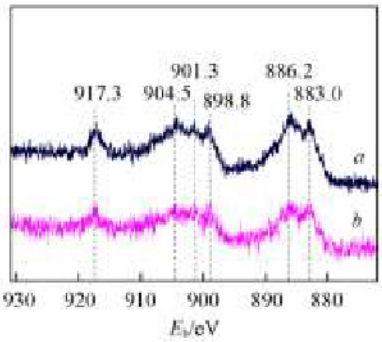

Fig.10 XPS spectra of Ce_{3d} region of catalysts

a. PdCe/CNT200; *b*. PDcE/CNT350.

4 Conclusions

Cerium-modified Pd catalysts exhibit high catalytic activities and good poison resistances for methanol electro-oxidation. The high catalytic activities are due to the synergistic interaction between palladium and cerium oxides/hydroxides. The good poison resistances of cerium-modified Pd catalysts are attributed to the poison-removal ability of cerium oxides/hydroxides. High-valence cerium oxides/hydroxides inhibit the accumulation of carbonaceous intermediates on the active sites of cerium-modified Pd catalysts.

References

[1] Bianchini C., Shen P. K., *Chem. Rev.*, **2009**, *109*(9), 4183
[2] Antolini E., Gonzalez E. R., *J. Power Sources*, **2010**, *195*(11), 3431
[3] Brouzgou A., Podias A., Tsiakaras P., *J. Appl. Electrochem.*, **2013**, *43*(2), 119
[4] Kamarudin M. Z. F., Kamarudin S. K., Masdar M. S., Daud W. R. W., *Int. J. Hydrogen Energy*, **2013**, *38*(22), 9438
[5] Feng Y., Bin D., Yan B., Du Y., Majima T., Zhou W., *J. Colloid Interf. Sci.*, **2017**, *493*, 190
[6] Zhu C., Wen D., Oschatz M., Holzschuh M., Liu W., Herrmann A. K., Simon F., Kaskel S., Eychmüller A., *Small*, **2015**, *11*(12), 1430
[7] Luo L. M., Zhang R. H., Chen D., Hu Q. Y., Zhang X., Yang C. Y., Zhou X. W., *Electrochim. Acta*, **2018**, *259*, 284
[8] Shen S., Guo Y., Luo L., Li F., Li L., Wei G., Yin J., Ke C., Zhang J., *J. Phys. Chem. C*, **2018**, *122*(3), 1604
[9] Chen Y., Chen M., Shi J., Yang J., Fan Y., *Int. J. Hydrogen Energy*, **2016**, *41*(38), 17112
[10] Yang Z. S., Wu J. J., *Fuel Cells*, **2012**, *12*(3), 420
[11] Fathirad F., Mostafavi A., Afzali D., *Int. J. Hydrogen Energy*, **2017**, *42*(5), 3215
[12] Kakati N., Maiti J., Lee S. H., Yoon Y. S., *Int. J. Hydrogen Energy*, **2012**, *37*(24), 19055

[13] Ma L., He H., Hsu A., Chen R., *J. Power Sources*, **2013**, *241*, 696
[14] Zhang K., Bin D., Yang B., Wang C., Ren F., Du Y., *Nanoscale*, **2015**, *7*, 12445
[15] Hao Y., Shen J., Wang X., Yuan J., Shao Y., Niu L., Huang S., *Int. J. Hydrogen Energy*, **2016**, *41*(4), 3015
[16] Cui X., Wang X., Xu X., Yang S., Wang Y., *Electrochim. Acta*, **2018**, *260*, 47
[17] Jurzinsky T., Kintzel B., Bär R., Cremers C., Tübke J., *J. Electroanal. Chem.*, **2016**, *776*, 49
[18] Peng C., Yang W., Wu E., Ma Y., Zheng Y., Nie Y., Zhang H., Xu J., *J. Alloy. Compd.*, **2017**, *698*, 250
[19] Zhang K. F., Guo D. J., Liu X., Li J., Li H. L., Su Z. X., *J. Power Sources*, **2006**, *162*(2), 1077
[20] Xu M. W., Gao G. Y., Zhou W. J., Zhang K. F., Li H. L., *J. Power Sources*, **2008**, *175*(1), 217
[21] Ou D. R., Mori T., Togasaki H., Takahashi M., Ye F., Drennan J., *Langmuir*, **2011**, *27*(7), 3859
[22] Scibioh M. A., Kim S. K., Cho E. A., Lim T. H., Hong S. A., Ha H. Y., *Appl. Catal. B*, **2008**, *84*(3/4), 773
[23] Guo D. J., Jing Z. H., *J. Power Sources*, **2010**, *195*(12), 3802
[24] Guo J. W., Zhao T. S., Prabhuram J., Chen R., Wong C. W., *J. Power Sources*, **2006**, *156*(2), 345
[25] Ye K. H., Zhou S. A., Zhu X. C., Xu C. W., Shen P. K., *Electrochim. Acta*, **2013**, *90*, 108
[26] Xu C., Tian Z., Shen P., Jiang S. P., *Electrochim. Acta*, **2008**, *53*(5), 2610
[27] Sun Z., Wang X., Liu Z., Zhang H., Yu P., Mao L., *Langmuir*, **2010**, *26*(14), 12383
[28] Zhou Z., Wang S., Zhou W., Wang G., Jiang L., Li W., Song S., Liu J., Sun G., Xin Q., *Chem. Commun.*, **2003**, 394
[29] Radmilović V., Gasteiger H. A., Ross P. N., *J. Catal.*, **1995**, *154*(1), 98
[30] Zhou Y., Gao Y., Liu Y., Liu J., *J. Power Sources*, **2010**, *195*(6), 1605
[31] Tauster S. J., Fung S. C., Baker R. T. K., Horsley J. A., *Science*, **1981**, *211*, 1121
[32] Tauster S. J., Fung S. C., *J. Catal.*, **1978**, *55*(1), 29
[33] Otomo J., Li X., Kobayashi T., Wen C., Nagamoto H., Takahashi H., *J. Electroanal. Chem.*, **2004**, *573*(1), 99
[34] Mueller J. T. , Urban P. M., *J. Power Sources*, **1998**, *75*(1), 139
[35] Müller J. T., Urban P. M., Hölderich W. F., *J. Power Sources*, **1999**, *84*(2), 157
[36] Hsing I. M., Wang X., Leng Y. J., *J. Electrochem. Soc.*, **2002**, *149*(5), A615
[37] Li K., Zhao P., *Mater. Res. Bull.*, **2010**, *45*(2), 243
[38] Wang S., Gu F., Li C., Cao H., *J. Cryst. Growth*, **2007**, *307*(2), 386
[39] Yu S., Liu Q., Yang W., Han K., Wang Z., Zhu H., *Electrochim. Acta*, **2013**, *94*, 245